



### **Coordinating Lead Authors**

Ramesh K. Vellore, Indian Institute of Tropical Meteorology (IITM-MoES), Pune, India,  
e-mail: [rameshv@tropmet.res.in](mailto:rameshv@tropmet.res.in) (corresponding author)

Nayana Deshpande, Indian Institute of Tropical Meteorology (IITM-MoES), Pune, India

### **Lead Authors**

P. Priya, Indian Institute of Tropical Meteorology (IITM-MoES), Pune, India

Bhupendra B. Singh, Indian Institute of Tropical Meteorology (IITM-MoES), Pune, India

Jagat Bisht, Indian Institute of Tropical Meteorology (IITM-MoES), Pune, India; Japan Agency for Marine  
Earth Science Technology (JAMSTEC), Yokohama, Japan

### **Review Editor**

Subimal Ghosh, Indian Institute of Technology Bombay, Mumbai, India

### **Corresponding Author**

Ramesh K. Vellore, Indian Institute of Tropical Meteorology (IITM-MoES), Pune, India,  
e-mail: [rameshv@tropmet.res.in](mailto:rameshv@tropmet.res.in)

## Key Messages

- Long-term observations (1951–2018) indicate a significant reduction in annual frequency of tropical cyclones (TCs) in the North Indian Ocean (NIO) basin [−0.23 per decade over the entire NIO; −0.26 per decade over the Bay of Bengal]. A significant rise [+0.86 per decade] in the frequency of post-monsoon (October–December) season very severe cyclonic storms (VSCS) is observed in the NIO during the past two decades (2000–2018) (high confidence).
- Observations indicate that frequency of extremely severe cyclonic storms (ESCS) over the Arabian Sea has increased during the post-monsoon seasons of 1998–2018 (high confidence). There is medium confidence in attributing this observed increase to human-induced SST warming.
- Analyses from the observations show a decline in number of thunderstorm days (1981–2010 relative to 1950–1980) by 34% over the Indian region, while there is a rise in short-span high-intensity rain occurrences (mini-cloudbursts) along the west coast of India (5 per decade) and along the foothills of western Himalayas (1 per decade) during the 1969–2015 period (high confidence).
- Climate model simulations project a rise in TC intensity (medium confidence) and TC precipitation intensity (medium-to-high confidence) in the NIO basin.

## 8.1 Introduction

High-impact weather phenomena associated with cyclonic storms (synoptic-scale weather disturbances that last for a few days), thunderstorms (occur on less than a day time scale), and short-lived cloudbursts (a time scale of few hours) that can produce intense rainfall amounts are generally categorized as severe or extreme weather events in the Indian weather chronology. The extreme weather events over the Indian region have profound socio-economic implications (e.g., De et al. 2005). The North Indian Ocean (NIO) rim countries (India, Bangladesh, Myanmar, Sri Lanka, Oman; countries within the Equator region—30° N; 50–100° E) comprising large coastal areas are severely affected by tropical cyclones (TCs) every year (see Singh et al. 2016; Ramsay 2017; Mohapatra et al. 2014, 2017). For example, the year 2018 witnessed four very severe TCs over this region during the pre-monsoon (March–May) and post-monsoon (October–December) seasons of India [Mekunu and Luban over the Arabian Sea (AS) in May and October 2018, Titli and Gaja in October

and November 2018 over the Bay of Bengal (BOB)]; Source: Annual cyclone review report, India Meteorological Department (IMD); see also Table 8.2].

Convective storms such as thunderstorms in general are considered as hazard to aviation, and also cause severe loss to life, agriculture, and property. The eastern and north-eastern states of India (West Bengal, Bihar, Assam, Chhattisgarh, Jharkhand, and Orissa) and adjoining regions in Bangladesh experience violent thunderstorms known as “Nor’wester” during the pre-monsoon season (Mukhopadhyay et al. 2005; Ghosh et al. 2008; Tyagi et al. 2012). Rainfall occurrences of unprecedented intensity have also been witnessed in the recent decades during the Indian summer monsoon (ISM; June–September) season. For example, heavy downpour that caused calamitous floods and heavy casualties in Mumbai during July 2005 (Bohra et al. 2006), in Leh of the trans-Himalayan region during August 2010 (Thayyen et al. 2013; Rasmussen and Houze 2012), in the northern states of Uttarakhand and Jammu and Kashmir during June 2013 and September 2014 (Lotus 2015; Ranalkar et al. 2016; Vellore et al. 2016, 2019; Priya et al. 2017), and in the southern state of Kerala during August 2018 (Mishra and Shah 2018) are to name a few. Various synoptic-scale signatures have been recognized in connection with these extreme rain situations, viz localized convective instabilities, large-scale organized monsoon activity and anomalous extratropical circulation, and their interactions with the monsoon circulation across the Himalayas (e.g., Vellore et al. 2014, 2016; see also Krishnan et al. 2019). The aforesaid extreme storm phenomena are significant threat to lives, property, and agricultural yields and cause huge revenue losses for the Indian subcontinent every year. It is also noteworthy to mention that extreme rain situations over the Indian subcontinent exhibit significant variations on a regional scale (Guhathakurta et al. 2011). A list of extreme rain events occurred in the recent times that resulted in calamitous flood situations over the Indian region is documented in Table 6.4. Long-term observations show significant rising trends in the frequency and magnitude of extreme rain occurrences over the ISM core rain-fed regions of central India during the later half of the twentieth century (Goswami et al. 2006) in an unequivocally warming climate (IPCC 2007, 2014; see also Krishnan et al. 2016; Singh et al. 2019).

Nonetheless, a clear deciphering of anthropogenic climate change manifestations on extreme rain or storm occurrences broadly remains elusive. Greater challenges are with detection and attribution of trends in high-impact rain events due to representation constraints of finer scale physical processes in the state-of-the-art climate modeling systems, as opposed to challenges in understanding of changes in large-scale environment in a warming climate (Mukherjee et al. 2018;

**Table 8.1** Classification of cyclonic disturbances observed in the NIO region and definition of cloudbursts referenced in this study

| Classification of cyclonic disturbance | Maximum sustained surface wind speed (MSW) |                    | Number of closed isobars (2 hPa interval) | Dvorak intensity (category) |
|--|--|--------------------|---|-----------------------------|
|  | Knots                                      | km h <sup>-1</sup> |   |                             |
| Low-pressure area                      | <17  | <31                | 1   | 1                           |
| Depression (D)                         | 17–27                                      | 31–50              | 2   | 1.5                         |
| Deep depression (DD)                   | 28–33                                      | 51–62              | 3   | 2                           |
| Cyclonic storm (CS)                    | 34–47                                      | 63–88              | 4–7                                       | 2.5–3                       |
| Severe cyclonic storm (SCS)            | 48–63                                      | 89–117             | 8–10                                      | 3.5                         |
| Very severe cyclonic storm (VSCS)      | 64–89                                      | 118–165            | 11–25                                     | 4–5                         |
| Extremely severe cyclonic storm (ESCS) | 90–119                                     | 166–221            | 26–39                                     | 5–6                         |
| Super cyclonic storm (SuCS)            | ≥ 120                                      | ≥ 222              | 40 or more                                | 6.5                         |
| Classification of cloudbursts          | Surface rainfall amount                    |                    |   |                             |
| Cloudburst                             | >100 mm in an hour                         |                    |   |                             |
| Mini-cloudburst                        | >50 mm in two consecutive hours            |                    |   |                             |

Source IMD (2003), Dvorak (1984), Velden et al. (2006), Deshpande et al. (2018)

The categories CS, SCS, VSCS, ESCS, SuCS described in the table are generally referenced as TCs in this chapter

Knutson et al. 2019a, b). Furthermore, projections of synoptic-scale TCs, mesoscale convective storms or thunderstorms (e.g., Tyagi et al. 2012), and very short-lived cloudburst occurrences (Deshpande et al. 2018) into the future from modeling framework are an ambitiously demanding task due to stringent model constraints in reproducing their occurrences on localized scale settings. Notwithstanding these challenges, considerable progress has been generally realized in the understanding of changes in TC activity over the global ocean basins (Walsh et al. 2016; Knutson et al. 2019a, b). The understanding of changes in regional-scale extreme or convective storm phenomena over the Indian subcontinent is still rudimentary. In this chapter, we present an assessment of occurrences and changes in extreme storm categories suitable for the Indian subcontinent.

intensity of maximum sustained surface wind speeds (MSW), and a classification of storm categories is given in Table 8.1. The gusty winds from the categories severe cyclonic storm (SCS) and above have larger devastating potential to life and property.

The category 4 and above TCs observed in the NIO region from the year 2000 during the cyclone seasons are given in Table 8.2. Various studies in the past have documented the long-term trends in frequency and intensity of NIO TCs (e.g., Raghavendra 1973; Mooley 1980; Mooley and Mohile 1984; Singh and Khan 1999; Raghavan and Rajesh 2003; Singh 2007; Niyas et al. 2009; Sikka 2006; Mohanty et al. 2010, 2012; Mohapatra et al. 2012, 2014; Gupta et al. 2018). In continuation with the past literatures, an update of historical and projected changes in TC intensity and frequency is documented in the following.

## 8.2 Synoptic-Scale Extreme Storms

TCs are synoptic-scale, warm-core, non-frontal low-pressure systems embedded in a weakly sheared environment over tropical warm waters characterized by organized convection within a closed cyclonic circulation (see Gray 1968; Anthes 1982; IMD 2003). The NIO basin typically contributes about 7–10% of world's TCs, and these TCs are further considered to be the most deadly ones in the world (e.g., Mohapatra et al. 2014; Sahoo and Bhaskaran 2016; Gupta et al. 2018). The India Meteorological Department (IMD) classifies NIO TC activity into different storm categories based on the

### 8.2.1 Historical Changes

Based on long-term (1891–2018) TC datasets, there were 1433 synoptic-scale cyclonic disturbances observed in the NIO basin on annual scale (Source: Cyclone eAtlas, IMD; <http://www.rmchennaieatlas.tn.nic.in>). Of which 55%, 24%, and 21% of these disturbances were characterized as D, CS, and SCS (see Table 8.1 for the classification), respectively. The TC contribution from BOB [AS] is about 80% [20%] in the NIO basin on annual scale. Also, a major percentage of cyclonic disturbances evolve to SCS and

**Table 8.2** Extreme category (category 4 and above; see Table 8.1) pre- and post-monsoon TCs observed over the Indian seas during the period 2000–2018

| Year | Category—basin—month—name of the storm                      |
|------|---|
| 2000 | VSCS—BOB—Nov—BB 05; VSCS—BOB—Dec—BB 06                      |
| 2001 | ESCS—AS—May—ARB 01  |
| 2003 | VSCS—BOB—May—BB 01  |
| 2004 | VSCS—BOB—May—BB 02  |
| 2006 | VSCS—BOB—Apr—Mala   |
| 2007 | VSCS—BOB—Nov—Sidr   |
| 2008 | ESCS—BOB—Apr—Nargis   |
| 2010 | ESCS—BOB—Oct—Giri   |
| 2011 | VSCS—BOB—Dec—Thane  |
| 2013 | ESCS—BOB—Oct—Phailin; VSCS—BOB—Nov—Lehar; VSCS—BOB—Dec—Madi |
| 2014 | ESCS—BOB—Oct—Hudhud; ESCS—AS—Oct—Nilofar                    |
| 2015 | ESCS—AS—Oct—Chapala; ESCS—AS—Nov—Megh                       |
| 2016 | VSCS—BOB—Dec—Vardah   |
| 2017 | VSCS—BOB—Nov—Ockhi  |
| 2018 | ESCS—AS—May—Mekunu; VSCS—AS—Oct—Luban; VSCS—BOB—Oct—Titli   |

Source IMD

**Table 8.3** Number of CS and SCS observed in the NIO basin during pre-monsoon (March–May; MAM) and post-monsoon (October–December; OND) seasons for the period 1891–2018

| Storm category | Ocean basin | Pre-monsoon (MAM) | Post-monsoon (OND) | Annual |
|----------------|-------------|-------------------|--------------------|--------|
| CS             | NIO         | 47 (14%)          | 149 (44%)          | 339    |
|                | BOB         | 37 (13%)          | 124 (43%)          | 286    |
|                | AS          | 10 (19%)          | 25 (47%)           | 53     |
| SCS            | NIO         | 82 (27%)          | 171 (56%)          | 307    |
|                | BOB         | 58 (25%)          | 141 (60%)          | 234    |
|                | AS          | 24 (33%)          | 30 (41%)           | 73     |

Source Cyclone eAtlas IMD

The numbers during pre- and post-monsoon seasons with respect to annual frequency are shown in percent

above categories during the pre-monsoon (March–May) and post-monsoon (October–December) seasons. Table 8.3 shows the number of synoptic-scale cyclonic storms observed in the NIO basin during the pre- and post-monsoon seasons. Note that, 56% [27%] of annually observed storms of severe category is seen in the NIO basin during the post-monsoon [pre-monsoon] season. On annual scale, 286 [53] CS and 234 [73] SCS were observed from the BOB [AS] during the 1891–2018 period.

Figure 8.1 shows the observed monthly frequency of CS and SCS for the period 1891–2018. The TC activity in the NIO basin exhibits a bimodal distribution with larger number of occurrences during the pre-monsoon and post-monsoon seasons (see also Haggag et al. 2010; Mohapatra et al. 2017). Notice that large number of CS formation is observed during the months of October and November in BOB and AS. A maximum of 72 [20] SCS events is observed during November [May] in BOB [AS] (see also Singh et al. 2016). The larger number of TCs in

BOB is possibly due to prevalence of upper-ocean warm stratification and higher sea-surface temperatures (SSTs) as compared to AS. The TC frequency in BOB constantly poses serious threat to eastern coastal Indian states Orissa, Andhra Pradesh, and Tamil Nadu. Mishra (2014) indicates that uneven surface temperature rise in the coastal regions during the recent decades also appears to have a bearing on increased cyclone vulnerability in these states. On average, about 5–6 TCs are generally observed in BOB and AS every year, of which 2–3 reach severe stages (Mohapatra et al. 2014). Based on long-period records, Tyagi et al. (2010) also indicated that more than 60% of BOB TCs endure landfall in various parts of the Indian east coast, 30% experience recurvature and landfall over Bangladesh and Myanmar, while 10% generally dissipate over the oceanic regions.

Large vertical wind shear during the ISM season generally prevents the formation of TCs. However, the ISM month of August during the 1891–2018 period witnessed a

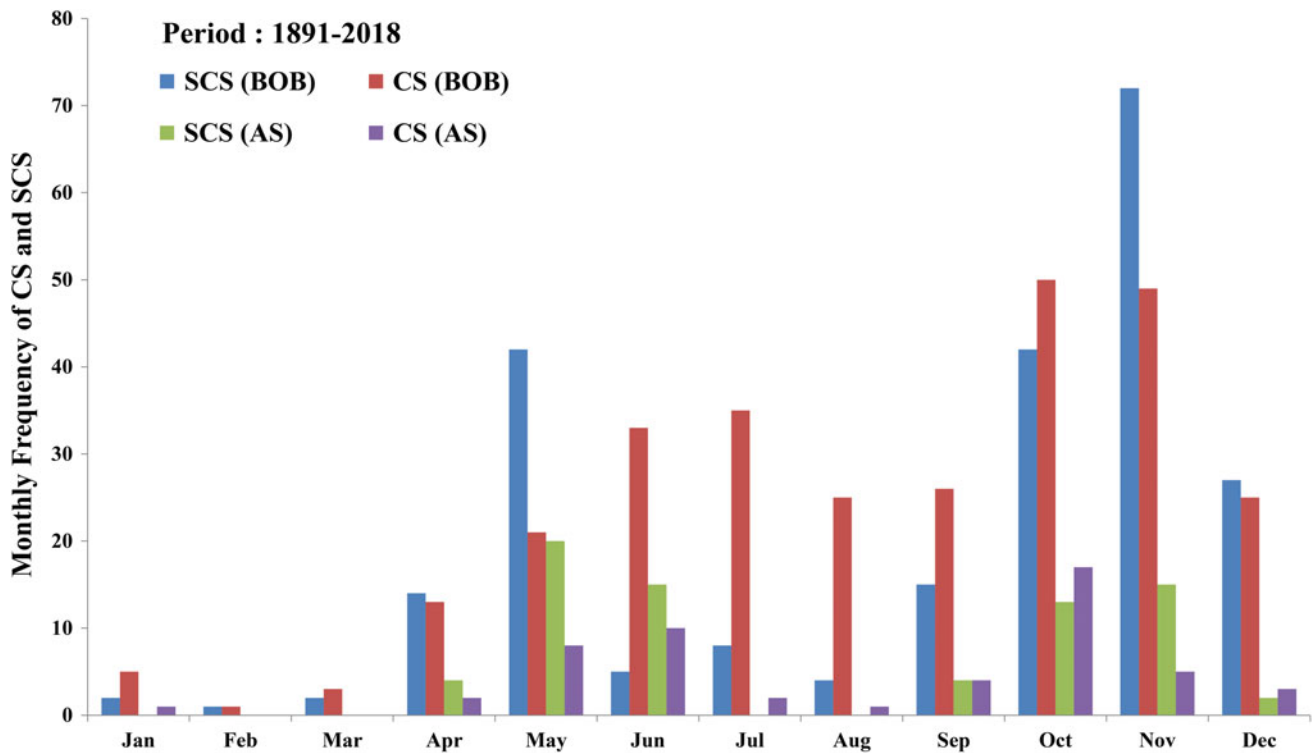


**Fig. 8.1** Observed monthly frequency of CS and SCS in the NIO basin during the 1891–2018 period. *Source* Cyclone eAtlas IMD; <http://www.rmcchennaicatlas.tn.nic.in>. BOB = Bay of Bengal, AS = Arabian Sea

maximum number of cyclonic disturbances in the BOB region which evolved into depression (D) category, i.e., 74 in June, 106 in July, 152 in August, and 125 in September, while the month of June witnessed a maximum number of 28 depressions in the AS region (For more details, see also Chap. 7; see also Singh et al. 2016; see also Prajeesh et al. 2013; Hunt et al. 2016).

A comparison between pre-1950 and the post-1950 (commonly referred to as the warming era) periods indicates that there is a rise in number of SCS from 94 to 140 (i.e., 49% rise) in the BOB region, and from 29 to 44 (i.e., 52% rise) in the AS region on annual scale. On seasonal scale, there is a rise in number of SCS from 93 to 160 (72% rise) in the NIO basin—of which there is a marked increase of +105% [+21%] observed during the post-monsoon [pre-monsoon] season. A consistent rise in number of SCS in the BOB region is noted irrespective of pre- or post-monsoon cyclone seasons, i.e., +100% [+42%] rise in the number of SCS in the aforesaid comparison periods during the post-monsoon [pre-monsoon] seasons of 1891–2018. On the contrary, there is a 15% reduction in the number of SCS in the AS region during the pre-monsoon season, while there is a 130% rise during the post-monsoon season (see also Mohanty et al. 2012; Singh et al. 2016 who also considered long-period TC records in their

assessments). The mean life period of SCS is estimated to be about 4 days, 6 days, and more for the extreme TC categories during the cyclone seasons. In particular, severe storm categories (VSCS and SuCS; see Table 8.1) show longer life period over AS [BOB] during pre-monsoon [post-monsoon] seasons (Kumar et al. 2017).

Figure 8.2 and Table 8.4 show the frequency distribution of TCs observed in the NIO region and trends in the frequency of CS and SCS, respectively, for the period 1891–2018. One can clearly see inter-annual and inter-decadal variability in the frequency distribution (Fig. 8.4). There is a significant decline in the annual frequency of NIO TCs, i.e.,  $-0.18$  per decade (1891–2018), and  $-0.23$  per decade (1951–2018) (see also Singh et al. 2000, 2001; Singh 2007; Mohapatra et al. 2014, 2017). While there is a significant upward trend ( $+0.07$  per decade) in SCS observed in the NIO region during the post-monsoon seasons of 1891–2018, there is a significant decline in the annual frequency of CS and SCS in the BOB region during the 1951–2018 period with trend values of  $-0.26$  per decade and  $-0.15$  per decade for CS and SCS, respectively. There is also an upward trend of CS and SCS observed in the AS region both on annual and seasonal scales during the 1951–2018 period, with larger trend values ( $+0.02$  per decade;  $<90\%$  confidence level) during the post-monsoon season. Further, these long-term

**Fig. 8.2** Observed annual frequency of **a** CS and above **b** SCS in the NIO. Linear trend lines are indicated by dashed lines —black (1891–2018), blue (1951–2018), red (2000–2018). Also, 10-year running mean is shown by a solid-green line. *Source* IMD

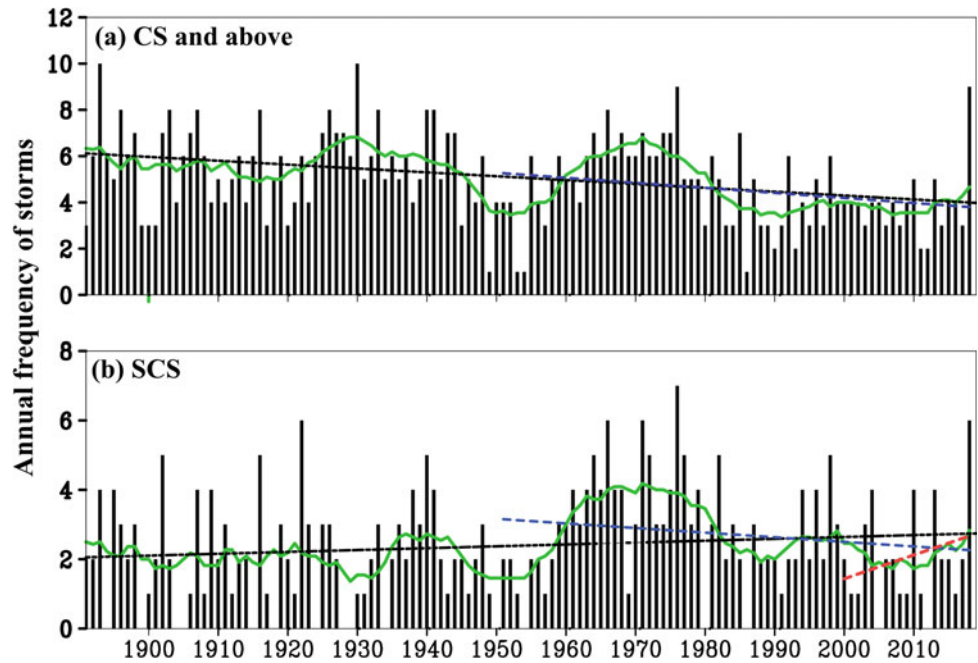


**Table 8.4** Linear trend (per decade) in frequency of CS and SCS observed in the NIO region based on the 1951–2018 and 1891–2018 periods

| Basin | Annual/season | Trend in CS   |               | Trend in SCS (VSCS)      |               |
|-------|---------------|---------------|---------------|--------------------------|---------------|
|       |               | 1951–2018     | 1891–2018     | 1951–2018 (2000–2018)    | 1891–2018     |
| NIO   | Annual        | <b>-0.231</b> | <b>-0.180</b> | -0.140 (+0.590)          | +0.050        |
|       | MAM           | -0.034        | -0.002        | -0.041 (-0.230)          | -0.004        |
|       | OND           | -0.065        | +0.011        | -0.072 ( <b>+0.860</b> ) | <b>+0.070</b> |
| BOB   | Annual        | <b>-0.264</b> | <b>-0.190</b> | <b>-0.154</b>            | +0.036        |
|       | MAM           | -0.035        | -0.001        | -0.040                   | +0.005        |
|       | OND           | -0.100        | +0.002        | -0.085                   | <b>+0.060</b> |
| AS    | Annual        | +0.045        | +0.020        | +0.021                   | +0.020        |
|       | MAM           | +0.002        | -0.000        | -0.001                   | -0.010        |
|       | OND           | +0.023        | -0.001        | +0.013                   | +0.020        |

*Source* Cyclone Atlas; IMD. Trends in VSCS occurrences (for the period 2000–2018) are shown in brackets. Confidence level above 90% is only shown in bold here

datasets also show a rising trend in TC frequency in the BOB region particularly during the months of November and May which is consistent with the earlier studies of Singh et al. (2000, 2007).

Further, based on IMD long-period datasets, Singh et al. (2000) identified a rise in intensification rates in the transformation of tropical disturbances into TCs and also a significant rise in SCS and VSCS in the NIO basin (see also Mohanty et al. 2012). Figure 8.3 shows the probabilities of TC intensification observed in the NIO basin, where one can notice that intensification probability from tropical depression D to CS [CS to SCS] is about 45% [48%] on annual scale. Also, there is a 21% [32%] probability of intensification from depression to extreme storm categories in the BOB [AS] region on annual scale. On seasonal scale, there

are higher probabilities of transformation observed during pre- and post-monsoon seasons, i.e., probability of transformation from D to CS is 72% and from CS to SCS is 64% during the pre-monsoon season, and 58% for D to CS and 53% for CS to SCS during the post-monsoon season. There is only a 27% probability for the transformations from D to CS and from CS to SCS during the ISM season. Although the number of storms in the AS region is relatively smaller than observed in the BOB region, the probabilities of transformation from [D to CS] CS to SCS are [33%] 27% larger in AS compared to BOB. While the translational speeds are larger for VSCS and SuCS categories (Chinchole and Mohapatra 2017; see also Kossin 2018), the intensification rates in the NIO basin were found to be rather pronounced in November during the post-monsoon season and

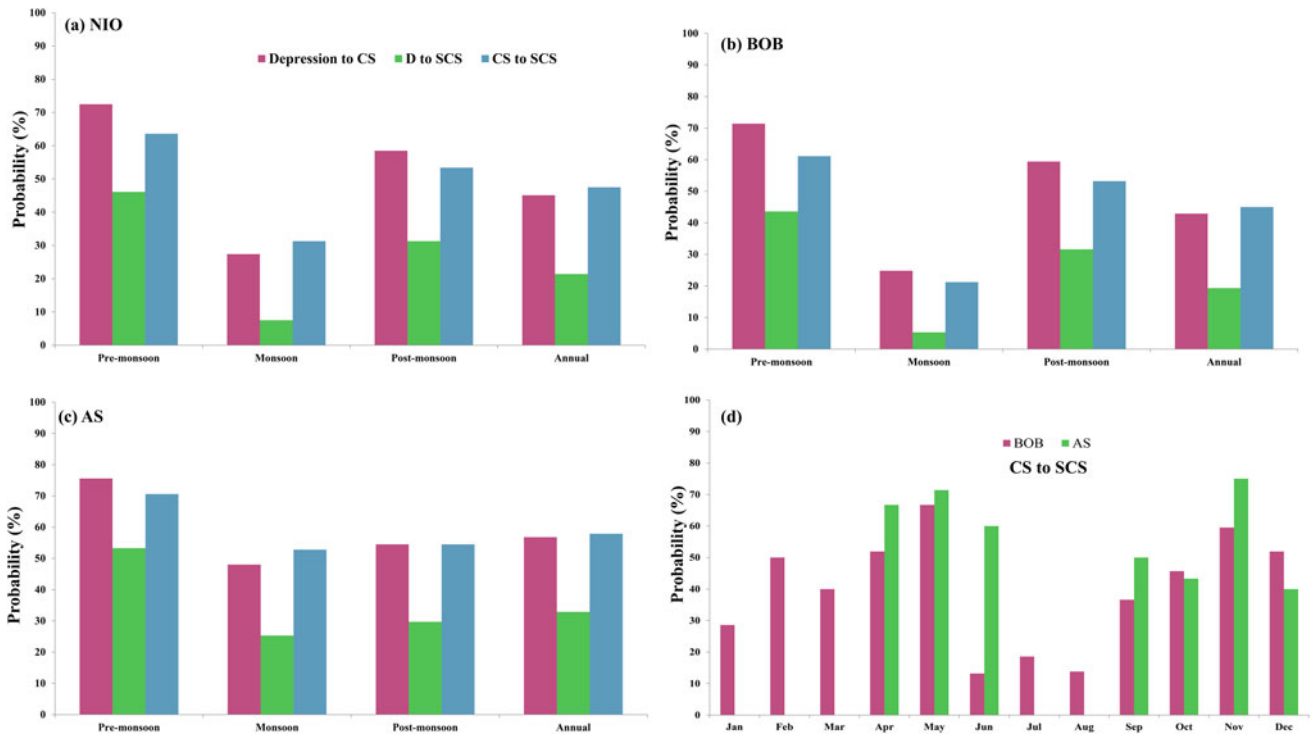
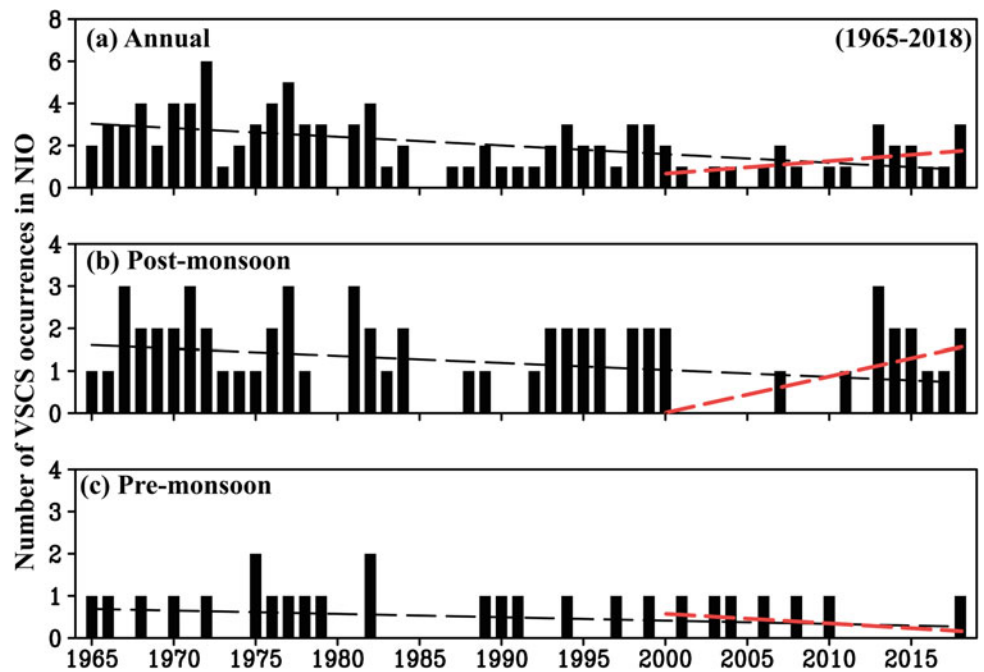


**Fig. 8.3** Probability of TC intensification (expressed in %) by seasons for the **a** NIO, **b** BOB, **c** AS, **d** by months in the BOB and AS region diagnosed for the period 1891–2018. *Source* Cyclone eAtlas IMD

**Fig. 8.4** **a** Annual and **b**, **c** seasonal VSCS occurrences in the NIO assessed for the period 1965–2018. Linear trend lines (black: 1965–2018, red: 2000–2018) are indicated by dashed lines. *Source* Mohapatra et al. (2014; IMD)



in May during pre-monsoon season (Fig. 8.3d). A few studies also indicate that the trends in TC intensity over the Atlantic Basin are more significant as compared to NIO which has been ascribed to inadequate observational records from the NIO region (Elsner et al. 2008; see also Walsh et al. 2016).

Figure 8.4 shows the observed number of VSCS occurrences from the NIO basin both on annual and seasonal scales based on the 1965–2018 period (see also Fig. 3 of Mohapatra et al. 2014). There were a total of 105 VSCS occurrences, of which 60% of them occurred during the post-monsoon season. There is a significant decline in the number of VSCS

**Table 8.5** Number of VSCS observed during the pre-monsoon and post-monsoon months in the BOB and AS regions for the period 1981–2018

| Basin | Pre-monsoon season | Post-monsoon season |
|-------|--------------------|---------------------|
| AS    | 6                  | 5                   |
| BOB   | 9                  | 28                  |

Source Balaji et al. (2018); Annual cyclone review reports, IMD

from 1960s—which is consistent with the analyses from earlier studies based on the long-term TC datasets (e.g., Mandal and Krishna 2009; Mohapatra et al. 2014).

However, a conspicuous rise in the VSCS is evident from the beginning of the twenty-first century (Fig. 8.4; Table 8.4). A linear trend analysis shows that the frequency of VSCS category storms significantly decreased at the rate of 0.41 per decade on annual scale, and on seasonal scale 0.17 [0.08] per decade during post-monsoon [pre-monsoon] season. Notably, there is a rising trend in VSCS (+0.59 per decade) seen in the NIO region during the 2000–2018 period which is dominated by significant upward trend in post-monsoon VSCS (+0.86 per decade) in the BOB region. Based on 1891–2018 period, there were about two VSCS (and higher intensity storms) occurrences per year in the NIO region on average—with predominance during the post-monsoon season.

Table 8.5 shows the number of VSCS occurrences observed in the BOB and AS regions during the pre-monsoon and post-monsoon seasons of 1981–2018. Note that on 40% of the occasions, the SCS in BOB transforms into VSCS during these cyclone seasons. There were 15 [6] extreme category storms documented in the BOB [AS] region between 2000 and 2018 during the cyclone seasons (Table 8.2). Clearly, a majority of SCS in the BOB region reaches VSCS and ESCS categories during these seasons. In particular, 6 out of 11 SCS in the AS region reached VSCS and ESCS (category 4 and above; see Table 8.2). There is also a detectable signal from the anthropogenic forcing which contributed to the increase in the frequency of VSCS and ESCS in the AS region during the post-monsoon season (Knutson et al. 2019a). Further, there is fivefold rise in the number of SCS in the AS region during the pre-monsoon season (2000–2018 relative to 1981–1999) while there is no notable change during the post-monsoon season. This is also consistent with the recent investigations of epochal variability in the reduction in vertical wind shear and also an increase in the pre-monsoon cyclone season span in favoring more TCs in the AS region (Wang et al. 2012; Rajeevan et al. 2013; Deo and Ganer 2014). In a recent study, Balaji et al. (2018) also indicated that there is a 34% rise in the frequency and also a 37% rise

in duration of VSCS category in the NIO region based on the 1997–2014 period dataset. A significant eastward shift was also noted in TC genesis locations in the BOB region during post-monsoon seasons of this period—which tends to enhance the vulnerability for the coastal regions of Bangladesh (see also Rao et al. 2019).

Various studies indicate the possible role of atmospheric and oceanic variability elements such as the Madden–Julian Oscillation (MJO), El Niño Southern Oscillation (ENSO), Indian Ocean Dipole (IOD), and Pacific Decadal Oscillation (PDO) in the variability of TC activity in the NIO basin. To name a few, Tsuboi and Takemi (2014) indicate that convectively active phase of MJO over the Indian Ocean facilitates more TC genesis episodes in the NIO region (see also Kikuchi and Wang 2010). ENSO years also tend to favor smaller number of post-monsoon cyclonic storms in the NIO region (Singh and Rout 1999). Sumesh and Kumar (2013) indicate that TC activity tends to be more [less] over the AS [BOB] region during the El Niño-Modoki instances, and suggest that concurrent occurrences of positive IOD and El Niño can significantly modulate the cyclogenesis parameters in the AS region as compared to El Niño-Modoki periods. Haggag et al. (2010) indicate that cold phase of PDO favors TC formation in the NIO region while the warm phase PDO suppresses the TC formation. In contrast, Girishkumar and Ravichandran (2012) and Girishkumar et al. (2015) indicate that accumulated cyclone energy from the BOB region is negatively correlated with the Niño 3.4 SST anomaly during October–December months, thereby enhancing the frequency, genesis, location, and intensity of TCs. In other words, negative IOD events and the La Niña years associated with warm phase PDO favor more TC activity in the BOB region. A few studies proposed a close relationship between SSTs and frequency of intense TCs (Singh et al. 2000; Hoyos et al. 2006). However, some studies (e.g., Pattanaik 2005; Sebastian and Behera 2015) differ from this view by suggesting that changes in SST alone are not adequate enough to establish the variability of TCs in the NIO region on different time scales, and these studies further emphasized on better understanding of large-scale atmospheric circulation and their links to TC variability in the NIO basin.



## 8.2.2 Climate Change Implications and Projected Changes

One of the serious concerns of climate change is the impacts of SST warming on frequency, intensity, and duration of TCs which remain elusive particularly for the tropical oceans (e.g., IPCC 2007, 2014; Elsner and Kocher 2000; Pielke 2005; Emanuel 2005; Anthes et al. 2006; Elsner et al. 2008; Xie et al. 2010; Knutson et al. 1998, 2010a, b; Ramesh Kumar and Sankar 2010). The NIO region witnessed a rapid rise in SSTs from 1950s by about 0.6 °C as compared to other tropical ocean basins (see Mohanty et al. 2012). Some of the earlier studies implied that changing SST trends and rising intense TCs in the NIO region may have consequences from anthropogenic climate change (e.g., Knutson et al. 2006; Elsner et al. 2008; Knutson et al. 2019b). Knutson et al. (2010b) also suggested that climate change signal to changes in SST and associated TC activity might emerge sooner in the Indian Ocean as compared to other ocean basins. Another potential concern in the NIO region is that TC intensities particularly in the AS region exhibit an unprecedented rise in the recent years (see Table 8.2). High-resolution global climate model experiments indicate that anthropogenic global warming has increased the probability of extremely severe cyclonic systems during the post-monsoon season in the AS region (Murakami et al. 2017). Although the investigations concerned with TC changes in the AS region are limited at this time, some recent studies suggest that increasing anthropogenic emissions of black carbon and sulfate can play a role in reducing the vertical wind shear so as to favor more intense TC activity in the AS region (Evan et al. 2011, 2012; Wang et al. 2012).

Many climate modeling investigations generally suggest that increasing or doubling of carbon dioxide (CO<sub>2</sub>) may enhance the frequency of severe/most intense cyclonic storms (e.g., Knutson et al. 2001; Knutson and Tuleya 2004; Webster et al. 2005; Oouchi et al. 2006; Bengtsson et al. 2007; Klotzbach and Landsea 2015). Some past studies such as Danard and Murthy (1989) and Yu and Wang (2009) pointed out that there could be an increase in TC frequency and TC intensity over the NIO basin in a doubled CO<sub>2</sub> world. Here, it is noteworthy to mention that there is a reasonable degree of sophistication in the current generation climate models that are capable of reproducing not only the salient features of TCs but also the associated dynamical–physical processes behind their development (e.g., Vidale et al. 2010). One can readily expect that warmer and wetter climate may favor more TCs with higher intensities from the climate change experiments using climate models. Despite that there is a consistency with the observed globally declining frequency of TCs in response to global warming

from these experiments (Sugi et al. 2002; McDonald et al. 2005; Yoshimura et al. 2006; Knutson et al. 2010a, 2019b), the inferences were rather dubious for basin-wide TC changes and more for the NIO region in particular (see also Zhao and Held 2012). Long-period trend assessment (International Panel on Climate Change Fifth Assessment Report—IPCC AR5; IPCC 2014) in surface air temperatures from climate model simulations, participated in CMIP5, for the historical periods indicates that there is a detectable warming signal over the Indian Ocean from the beginning of twentieth century. But, the present-day climate model assessments for the NIO region apparently present larger ambiguity due to larger bias in the simulations concerned with NIO TC activity—while there is a realistic agreement for TC frequency and intensity changes against observations for the Atlantic and Pacific Ocean basins (Zhao et al. 2009; Bender et al. 2010; Knutson et al. 2014). Further, the reduction in TC frequency over most part of the Indian Ocean appears to come from equal contributions of rising CO<sub>2</sub> emissions and anomalous SST patterns—notably, the SST effect and reduction in vertical shear have more precedence to the rising numbers of TCs in the AS region (Sugi et al. 2014).

Through the use of reanalyzed archives, Ramesh Kumar and Sankar (2010) indicate that the declining frequency of TCs in the NIO region in the historical period has no clear bearing global warming signal in association with the rising SSTs, but the warming signal may have greater impact on observed changes in atmospheric parameters such as decreasing mid-tropospheric relative humidity, low-level vorticity, and vertical wind shear during cyclone seasons of the NIO region (see also Pattanaik 2005; Sebastian and Behera 2015). In corroboration with these investigations, Balaguru et al. (2014) further indicate that intensity of major TCs in the BOB region during the post-monsoon season tends to have a coupled response from increasing upper-ocean content consistent with the rising SSTs and enhanced convective instability in the atmosphere. Murakami et al. (2017) performed a suite of high-resolution coupled model experiments and also showed that increasing anthropogenic-induced warming has potentially increased the probability of extreme category storms in the AS region, while the role of natural variability is rather minimal for the unprecedented rise in TC activity in the AS region.

As compared to other ocean basins, future changes in TC activity in the NIO region have received less attention in particular. As for the projected changes in TC activity in NIO region based on the investigations from climate change experiments, there is a large inconsistency noted in the projections from various state-of-the-art climate models. Knutson et al. (2010a, b) documented that in comparison with present-day changes, there is a large variation between

—52% (Oouchi et al. 2006) and +79% (Sugi et al. 2009) in the future changes in TC frequency (see Table S1 of Knutson et al. 2010a, b), and between −13 and +17% (Oouchi et al. 2006) for the changes in TC intensity. The ambiguities largely appear to arise from factors in the model architecture and representation of physical processes such as model resolution, choice of convection parameterization, as well as model-simulated SST changes. In addition, detecting TCs in climate models is also apparently a form of modeling uncertainty (see also Murakami et al. 2012a, b). There is a low confidence in the climate projections of rising annual frequency of VSCS (category 4 and above; see Table 8.1) at the end of twenty-first century in the NIO region (2081–2100 relative to 1981–2005). However, in a 2° anthropogenic warming scenario, there is a medium-to-high confidence in the projected rise in TC precipitation rates and intensities for the NIO region (Knutson et al. 2019b).

Murakami et al. (2014) also indicated that future changes in TC activity in the NIO region have larger dependence on future changes in thermodynamic factors (e.g., low-level relative humidity, SST anomalies) than future changes in dynamic factors (e.g., vertical wind shear, low-level vorticity, mid-level vertical velocities). High-resolution climate simulations show a scenario of increasing TC frequency by about 46% in the AS region, while there is a reduction by 31% in the BOB region, and the reduction [rise] is notably during pre-monsoon [post-monsoon] cyclone season (Murakami et al. 2013). The TC frequency is projected to decline in the AS and BOB regions during pre-monsoon season where the frequency change is influenced by aforesaid dynamical factors, while an east–west contrast (i.e., a reduction in BOB and rise in AS) is noted during the post-monsoon season where the future changes in aforesaid thermodynamic parameters may be of greater importance. There is also an attribution of southerly surge enhancements over the western AS and southern BOB regions during the post-monsoon cyclone season due to active inter-tropical convergence zone situations to the rising frequency of SCS in these regions (Mohanty et al. 2012). The reader is also referred to Walsh et al. (2016) and Knutson et al. (2019a, b) for a comprehensive documentation of climate change influences on TCs from various oceanic basins.

The IPCC—AR5 report published in 2014 (IPCC 2014) enunciates that “the confidence on attribution of changes in TC activity to human influences still is low owing to inadequate observational evidence and physical understanding of the anthropogenic drivers of climate and TC activity, i.e., there is a low confidence in basin-scale projections of changes in TC intensity and frequency of all basins.” Various recent studies indicate that the projected changes in global frequency of TCs will decrease while severe TCs (categories 4 and above; see Table 8.1) in anthropogenic warming world exhibit a general rise over the global ocean

basins, but the confidence from the information available till date is still debatable owing to the limited literature (see also Table 1 of Knutson et al. 2019a). Hitherto, scientific investigations only led to various contentions in reference to anthropogenic climate change and its connections to changes in TC activity pertinent to NIO region. However, Knutson et al. (2019a) describe that contribution of anthropogenic forcing signal to rising severe category TS in the AS region is rather not just coincidental, but there is a medium confidence based on available investigations till date. The latest assessment by Knutson et al. (2019b) provides a medium confidence to projected TC intensity rise and medium-to-high confidence to TC precipitation intensity in the NIO basin, while the confidence is yet low for the projected rise in the annual frequency of VSCS during the twenty-first century.

### 8.3 Localized Severe Storms

Localized severe weather outbreaks occurring on meso- $\gamma$  scale (on the spatial scale of 2–20 km, a few hours temporally; Orlanski 1975) in association with high winds, hail, thunder, lightning, etc., are generally categorized into severe convective storms. Some examples include thunderstorms, hail storms, dust storms, etc. Various studies (Manohar and Kesarkar 2005; Kandalgaonkar et al. 2005; Tyagi 2007; Kulkarni et al. 2009; Singh et al. 2011) have investigated the severe storm activity for the Indian region. Cloudbursts are a special class which falls under the short-lived intensely precipitating convective storms (see Table 8.1). These are predominant over the mountainous regions of northern part of India (Das et al. 2006; Dimri et al. 2017; Deshpande et al. 2018).

Thunderstorms are localized convective storms, which are more frequent at low latitudes, where there is a greater expediency of convective overturning occurrences in association with heated low-level atmospheric layers coming in contact with warm ground or water. Synoptic and meteorological conditions generally favorable for the occurrences of thunderstorm include conditional and convective instability in the atmosphere, ample supply of moisture at low levels, strong wind shear, and a dynamical mechanism (lifting or destabilization by advective processes) to release the instability present in the atmosphere (e.g., Doswell 2001; Bhardwaj and Singh 2018). Thunderstorms occur all through the year in different parts of India; however, their frequency and intensity are found to be maximum from March to May owing to prevalence of unstable atmospheric conditions and high temperatures at lower levels (Tyagi 2007; Singh et al. 2011; Saha et al. 2014; Das 2015b). The thunderstorm activity generally remains low during the mid-ISM months (July and August) throughout the country, whereas it is

pronounced during the onset and withdrawal phase months (June and September). The eastern and northeastern states of India (West Bengal, Bihar, Assam, Jharkhand, and Orissa) and Bangladesh experience a special type of violent thunderstorms known as “Nor’westers (also known as Kal-Baisakhi by the locals; Desai 1950)” during the pre-monsoon months (March–May). These storms are triggered by the intense convection activity over the Chhotanagpur Plateau (Jharkhand region) and are generally associated with sudden violent gusty winds from northwest, known as squalls, with wind speeds exceeding  $28 \text{ m s}^{-1}$ . These are usually accompanied with heavy rainfall (about  $100 \text{ mm h}^{-1}$ ) and oftentimes hail of sizes 30 mm in diameter, causing flash floods, severe property and agricultural damages (e.g., Chakrabarty et al. 2007; Pradhan et al. 2012).

Thunderstorm is always characterized by cumulonimbus cloud type, in which individual cells produce copious rains, and sometimes hail, strong winds, and even occasional tornadoes in northeast India and Bangladesh from Nor’westers, e.g., a F3 tornado (on the Fujita–Pearson scale) over Rajkanika block of Kendrapara district of Orissa, India, on 31 March 2009 (Litta et al. 2012). Over the southern and northeastern parts of India, the pre-monsoon thundershowers are called by various names in conjunction with rain favorable to local plantations, viz Tea showers in Assam, Mango showers in Kerala, Konkan, and Goa, and Coffee showers in Kerala. Thunderstorms in India generally fall under two categories: strong rains and maximum wind speeds ranging from  $8$  to  $20 \text{ m s}^{-1}$  with loud blasts of thunder and frequent lightning flashes in the category of moderate thunderstorms, while continuous thunder and lightning with strong rains and wind speeds  $>20 \text{ m s}^{-1}$  in the category of severe thunderstorms. The lightning activity from thunderstorms is also significantly noticeable despite lower values of convective available potential energy, over the northern, central India and Bangladesh as compared to other parts of Indian subcontinent (Murugavel et al. 2014). Based on the genesis and life cycle of thunderstorms, they are grouped into different types, viz single-cell thunderstorms (a single cloud cell moving independently without combining with any other cell with a life cycle of 30 min to 1 h, moves slowly with mean environmental wind, and generally the vertical wind shear is small), multiple-cell thunderstorms (consists of a series of evolving cells with a life cycle of 3–6 h, possible hail storms and damaging winds and isolated tornadoes and travel over a few hundreds of kilometers), and squall lines (a chain of thunderstorms connected together and moving like a single entity usually accompanied by high-speed winds). Regardless of the type of thunderstorms, they go through three stages: the cumulus stage, the mature stage, and the dissipation stage.

In addition, two types of high-impact dust storms known as “Andhi” co-occur with thunderstorms of northwest India

during the later part of the pre-monsoon season following the development of a heat low over this region. These dust storms are essentially thunderstorms in the arid regions of northwest India, where the local instability mechanisms are similar to thunderstorms and occur in association with large cumulus or cumulonimbus clouds (Raipal and Deka 1980; Middleton 1986). The first type is pressure-gradient dust storm which is characterized by higher temperatures and relatively low moisture content in the lowest atmospheric layers which makes the thunderstorms to have much higher cloud bases above the ground (3–4 km). On occasions, a strong pressure gradient develops to the south of the heat low causing strong winds lifting the dust and sand that are amply available in this region. Another type of dust storm is convective dust storm which develops in association with strong negatively buoyant downdraft of cumulonimbus cloud. The pressure-gradient dust storms generally last for longer periods with suspended dust in air, whereas convective dust storms last for a few minutes to few hours. The annual mean frequencies of Andhi are higher over the Indian states of Rajasthan, Punjab, Haryana, and Delhi. India is also among the countries in the world having large frequency of hail storms, associated with severe thunderstorms in association with multiple updrafts and downdrafts. These are more commonly seen along the Himalayan foothills causing severe large-scale agricultural damages (De et al. 2005). The frequency of hailstorms is small in winter; however, it increases from February and peaks during the pre-monsoon months (March and April). Hailstorms are rare during the ISM season. Unprecedented hailstorms lasting for a week or more are observed on occasions over north peninsular India (Kulkarni et al. 2015).

Generally, cloudburst is a severe weather outbreak feature commonly seen along the southern Himalayan slopes of the Indian subcontinent during the ISM months (Dimri et al. 2017; Deshpande et al. 2018). These are associated with thunderstorms where strong updrafts from intense vortices on smaller scale tend to hold up a large amount of water and upon sudden cessation results in catastrophic rainfall in a short period of time (greater than  $10 \text{ cm h}^{-1}$ ) concentrated over a limited geographical area (Bhan et al. 2004; Dimri et al. 2017; see references therein). Romatschke and Houze (2011) indicated that precipitation is predominantly associated with smaller spatial scale but highly convective systems along the western Himalayan region and bulk of the cloudburst episodes are observed between 1000 m and 2500 m elevations of the Greater Himalayas. Das et al. (2006) quote “Cloudbursts in India occur when monsoon clouds associated with low-pressure area travel northward from the Bay of Bengal across the Ganges Plains onto the Himalayas and ‘burst’ in heavy downpours.” For example, there were seven cloudburst instances witnessed over the western Himalayan state of Uttarakhand during the ISM season of 2018

(<https://sandrp.in/2018/07/21/uttrakhand-cloudburst-incidents-2018/>).

A comprehensive documentation of 30 instances of cloudbursts and associated damages in the Himalayas from 1970 is shown in Dimri et al. (2017). Several researchers also highlight the role of large-scale forcing and anomalous atmospheric circulation conditions leading to flood situations in and along the western Himalayas (e.g., Houze et al. 2011; Vellore et al. 2016) with implications to cloudburst instances though not directly. The modeling community observes large limitations to capture the cloudburst events due to outstanding issues such as understanding of microscale interactions with rugged and variable orography, paucity of observations, and representation of physical processes at a much-localized scale setting. The essentiality of more modeling studies with multiple events and observations for better understanding these severe convective events over the Himalayan region is also clearly suggested. Indian scientists have additionally coined another new term “mini-cloudbursts (more than 5 cm in two consecutive hours)” (Deshpande et al. 2018) to define incidences of heavy rains over short period of time. Instances include heavy rainfall in Mumbai during the ISM season, e.g., 944 mm rainfall on July 27, 2005, and 304 mm rainfall on September 20, 2017, that caused massive urban flood. The new definition distinguishes the cloudbursts associated with high topography (e.g., Leh event in August 2010; Uttarakhand event in June 2013) and rainfall incidences over the plain region exceeding  $10 \text{ cm h}^{-1}$  that can result in urban flooding. The aforesaid Mumbai events fall under mini-cloudburst classification.

### 8.3.1 Historical Changes

The thunderstorm data available for the Indian region has been comprehensively documented in the recent studies of Tyagi (2007), Bharadwaj et al. (2017), Bharadwaj and Singh (2018). Based on the compiled dataset, Fig. 8.5 shows the state-wise distribution of thunderstorm events over the Indian region during the 1978–2012 period. Five states (West Bengal, Orissa, Bihar, Assam, and Jharkhand) were the worst hit of thunderstorms in terms of fatalities, injuries, and casualties. West Bengal experienced most intense thunderstorm events and highest casualties during this period. Maharashtra and Kerala experienced 147 and 79 events, respectively, during this period, the fatalities and casualties are comparatively less in these states. Delhi experienced only seven events with significant injuries and casualties (Bhardwaj et al. 2017). Figure 8.6 shows mean number of thunderstorm days for different seasons over the Indian region for two periods 1951–1980 and 1981–2010. On the annual scale, high thunderstorm activity days (100 days or

more) are seen over northern Assam, Meghalaya, and West Bengal. The annual frequency of thunderstorm days latitudinally increases from lower to higher latitudes; however, there is a sharp decline in their frequency noticed from 1980s, i.e., during the 1981–2010 period, relative to 1951–1980 time period, there was 34% decline of frequency of thunderstorm days (Bhardwaj and Singh 2018; Singh and Bhardwaj 2019). The observed changes in thunderstorm activity are found to be mostly dependent upon latitude and season, and they are consistent with the seasonal migration of the inter-tropical convergence zone (ITCZ) and the solar heating of the Indian landmass (Manohar et al. 1999; Manohar and Kesarkar 2005) along with strong regional influences from the topography. The thunderstorm activity also exhibits an increasing number from the western side of the subcontinent and moves northeastwards toward the Himalayan foothills, and more notably the highest and lowest number of thunderstorm days are observed over the mountainous terrain of Jammu and Kashmir and Ladakh region, respectively. Over the Gangetic plains, West Bengal and surrounding regions record between 80 and 100 days of thunderstorm activity annually while Kerala records the highest (80–100 days) thunderstorm frequency over the peninsular regions of India (Tyagi 2007).

The pre-monsoon increase in thunderstorm activity is primarily attributed to the topography, insolation, and advection of moisture under favorable wind conditions. The spatial distribution of thunderstorm occurrences during pre-monsoon season indicates a maximum occurrence over the north, northeast, and southern parts of India (Fig. 8.6). The highest frequency of thunderstorms is noticed over the country during monsoon season as a whole, and mostly over the northern and northeastern parts of India. During the post-monsoon season, highest number of thunderstorms occurs over Kerala and the neighboring state of Tamil Nadu. Lowest number of thunderstorms over India is generally observed during the winter season due to stable and dry atmospheric conditions prevailing over most parts of the Indian subcontinent. The declining thunderstorm activity over the Indian subcontinent is suggestively attributed to reductions in rainfall activity and in the moisture amount, due to a fall in the frequency of monsoon depressions, and enhanced intensities of natural variability sources such as ENSO, and PDO. Also, a recent study notes that there is a decline in the dust loading of the atmosphere, or a decrease in intensity of dust storms, during the period 2000–2017 due to increasing pre-monsoon rains over the northwestern states and the Indo-Gangetic Plains (Pandey et al. 2017). Das (2015a) suggests that frequency of cloudburst events in the western Himalayan region has been on the continuous rise due to faster evaporation rates from glacial lakes at high altitudes, as a consequence of global warming. It is also noted that most of the cloudburst events are reported from

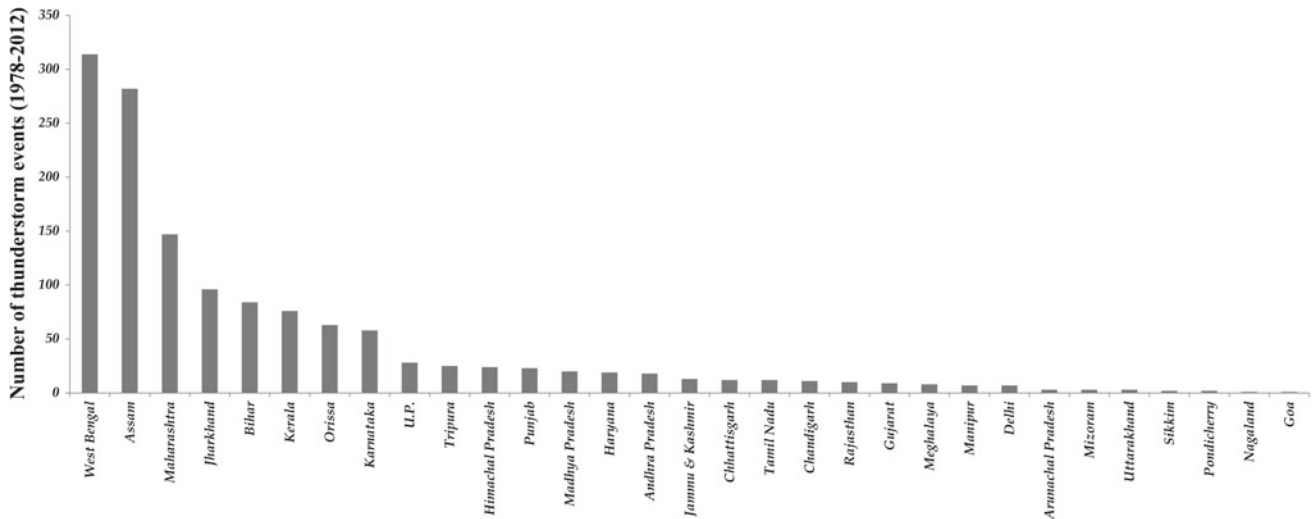


**Fig. 8.5** State-wise distribution of thunderstorm events in India for the period 1978–2012. *Source* IMD, see also Bharadwaj et al. (2017)

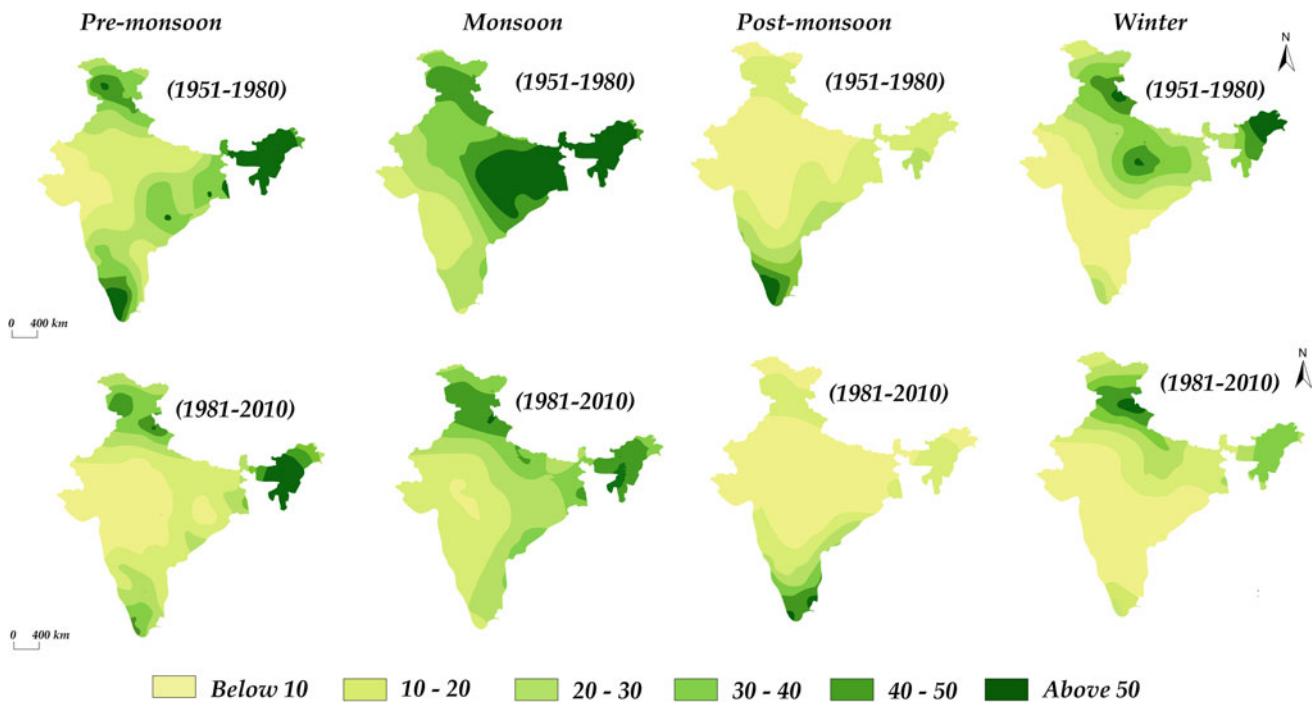


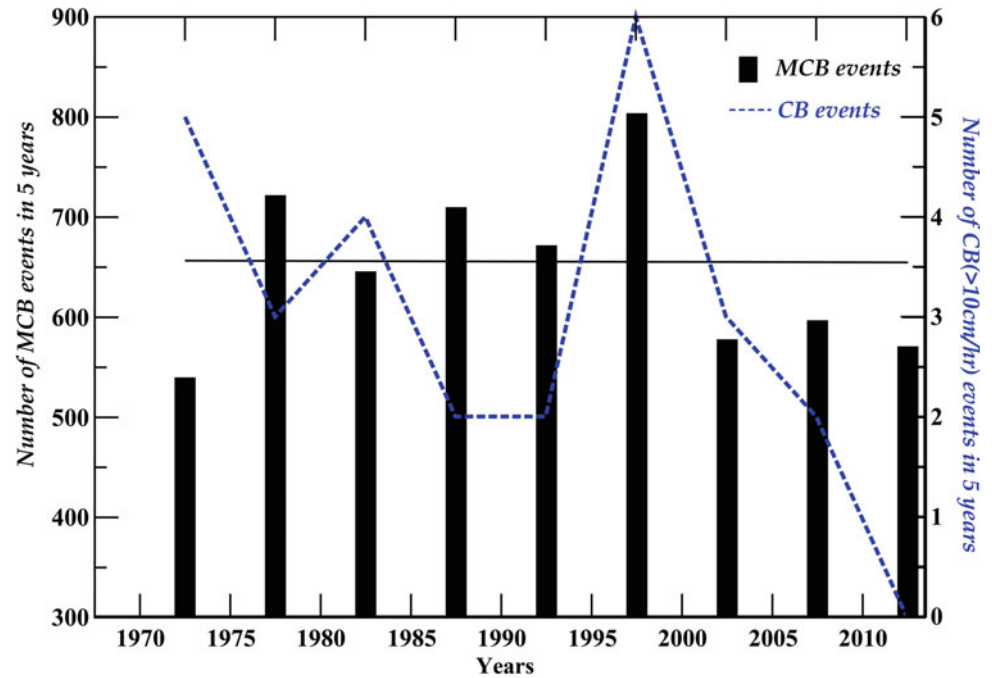
**Fig. 8.6** Number of thunderstorm days in India: mean frequency during different Indian seasons for the period 1951–1980 and 1981–2010. *Source* IMD; Adopted from Bharadwaj and Singh (2018) under CC BY-NC 4

ISM months, and the cloudburst events are found to have a dynamical sequence of convective triggering followed by orographic locking mechanisms (Dimri et al. 2017).

Figure 8.7 shows distribution of cloudburst (rainfall rate exceeding  $100 \text{ mm h}^{-1}$ ) and mini-cloudburst (rainfall in consecutive 2 h exceed 5 cm) events over the Indian subcontinent during the period 1969–2015. Based on the information from 126 station observations during this period, on an average, the Indian subcontinent experienced 130

mini-cloudburst events and 1 cloudburst event per year. During the ISM season, there are 2–3 mini-cloudburst events witnessed along the Himalayan foothills, west coast of India, Indo-Gangetic Plains and Saurashtra, and as high as five such events are noticed over the monsoon trough region of central India. The onset period of ISM typically witnesses more intense mini-cloudbursts (average rain intensities of 7 cm per event) prominent over the coastal regions of Gujarat and Odisha, and northeastern parts of India. Thus, a major part of

**Fig. 8.7** Annual (pentad) frequency of cloudburst (CB) and mini-cloudburst (MCB) events observed over the Indian subcontinent during the period 1969–2015. Data source India Meteorological Department; see also Deshpande et al. (2018)



Indian subcontinent receives rainfall amounts more than 6 cm from mini-cloudburst events during July–August months, and these events have been observed to be very intense over the eastern part of Indo-Gangetic plains during the withdrawal phase of ISM. Although short-lived cloudburst and mini-cloudburst occurrences are generally projected to decline in frequency (not statistically significant at 5%) (see Fig. 8.7), it is observed that there is a significant increase of in these events (1 per decade) along the Himalayan foothills and west coast of India (5 per decade), while decreasing over northeast India in the recent decades (Deshpande et al. 2018).

### 8.3.2 Projected Changes

It is generally correlated that the temperature increase associated with global climate change will lead to increased thunderstorm intensity and associated heavy precipitation events. As for the changes in severe convective storms (thunderstorms, hail storms, cloudbursts) due to climate variability and anthropogenic modifications of atmospheric environment, still there is “low confidence” in observed trends because of historical data inhomogeneities and inadequacies in monitoring systems. Projections of aforementioned severe weather outbreaks in the future are very difficult to pronounce at this time due to the indispensable need of enhancing the meso- $\gamma$  scale rainfall observational network and ultra-fine resolution model architecture with improved representations of physical processes (convective,

cloud-microphysics, aerosol-cloud interactive processes) (Singh et al. 2019). Therefore, the response of severe convective storms to changing climate is still open-ended and rapidly growing area of research around the world.

## 8.4 Knowledge Gaps

Though there is a rise in intensification rates in the transformation from tropical disturbances to severe category tropical storms over NIO basin, attribution of these changes to SST variability and environmental parameters are still not clear. In addition, inadequate long-term observational data, strong internal variability of the regional climate system, and limitations in realistically representing the multi-scale processes of TC evolution in climate models also add to the underlying uncertainty. Moreover, the climate simulations show a large spread ( $-52$  to  $+79\%$  relative to present-day changes) in the future projections of TC frequency in the NIO region (Knutson et al. 2010a, b). These factors demand for an improvement in the existing climate/Earth-system models and promising downscaling methods to reduce the uncertainties and to provide finer details of TC activity (see Knutson et al. 2015; see also Vishnu et al. 2019).

The attributions of trends in localized convective storms still have a low confidence owing to data inhomogeneities and insufficient monitoring systems, and the response of localized convective storms to changing climate still remains an open-ended research around the world.

## 8.5 Summary

A status on the current understanding of the changes in high-impact, in terms of socio-economic implications, stormy weather phenomena pertinent to the Indian subcontinent [i.e., severe category tropical cyclonic storms in the NIO region, thunderstorms and associated dust storms, short-span intense rain-producing cloudbursts] is documented in this chapter. Considerable progress has been generally realized in the understanding of changes in TC activity over the global ocean basins (see Walsh et al. 2016; Knutson et al. 2010a, 2019a, b), while a clear understanding of the reasoning behind the changes in NIO TC activity and extreme rain or convective storm occurrences over the Indian subcontinent is still rudimentary. Observed TC changes during the 1951–2018 (relative to pre-1950 period) period indicate that there is a rise in severe category TCs by 49% (relative to pre-1950 period) in the BOB region, and 52% in the AS region. There is also a marked rise of these storms in the NIO basin by 105% during the post-monsoon (October–December) season. There is a significant decline in the annual frequency of TCs in the NIO basin, i.e.,  $-0.23$  per decade for the entire NIO, and  $-0.26$  per decade for the BOB. Observations also indicate a rising trend in VSCS (category 4 and above TC; see Table 8.1) in the NIO region during the 2000–2018 period which is apparently controlled by the post-monsoon VSCS trend ( $+0.86$  per decade) from BOB. Another growing concern is the rising number and severe TCs in the AS region in the recent years—i.e., 6 out of 11 TCs formed in AS reached greater severity during the 2000–2018 period (see Table 8.2). Based on the investigations available till date for reasoning behind this rise, there is a consensus of medium confidence in attributing the observed rise in the AS post-monsoon TCs to human-induced SST warming (Murakami et al. 2017; Knutson et al. 2019a, b).

Localized convective storms such as thunderstorms over the Indian subcontinent indicate a declining frequency by 34% in the post-1980 period which is suggestively attributed to reductions in rainfall activity and in the moisture amount due to a fall in the frequency of monsoon depressions, and enhanced intensities of natural variability climate drivers. Although short-lived cloudburst and mini-cloudburst occurrences generally indicate a decline in frequency in the recent decades, it is observed that there is a significant increase in these events along the Himalayan foothills (1 per decade) and west coast of India (5 per decade).

## References

- Anthes RA (1982) Tropical cyclones: their evolution, structure and effects. Meteorological monograph No. 41. American Meteorological Society, 208 pp
- Anthes RA et al (2006) Comments on hurricanes and global warming—potential linkages and consequences. *Bull Am Met Soc* 87:623–628
- Balaguru K, Taraphdar S, Leung LR, Foltz GR (2014) Increase in the intensity of postmonsoon Bay of Bengal tropical cyclones. *Geophys Res Lett* 41:3594–3601
- Balaji M, Chakraborty A, Mandal M (2018) Changes in tropical cyclone activity in north Indian Ocean during satellite era (1981–2014). *Int J Climatol* 38:2819–2837
- Bender MA et al (2010) Modeled impact of anthropogenic warming of the frequency of intense Atlantic hurricanes. *Science* 327:454–458
- Bengtsson L et al (2007) How may tropical cyclones change in a warmer climate? *Tellus* 59:539–561
- Bhan SC, Paul S, Kharbanda KL (2004) Cloudbursts in Himachal Pradesh. *Mausam* 55:712–713
- Bhardwaj P, Singh O (2018) Spatial and temporal analysis of thunderstorm and rainfall activity over India. *Atmósfera* 31:255–284
- Bhardwaj P, Singh O, Kumar D (2017) Spatial and temporal variations in thunderstorm casualties over India. *Singap J Trop Geogr* 38:293–312
- Bohra AK et al (2006) Heavy rainfall episode over Mumbai on 26 July 2005: assessment of NWP guidance. *Curr Sci* 90:1188–1194
- Chakrabarty KK, Nath AK, Sengupta S (2007) Nor'wester over West Bengal and comfortability. *Mausam* 58:177–188
- Chinchole PS, Mohapatra M (2017) Some characteristics of translational speed of cyclonic disturbances over North Indian ocean in recent years. In: Tropical cyclone activity over the North Indian Ocean. Springer, Cham, pp 165–179
- Danard MTS, Murty TS (1989) Tropical cyclones in the Bay of Bengal and CO<sub>2</sub> warming. *Nat Hazards* 2:387–390
- Das PK (2015a) Global warming, glacial lakes and cloud burst events in Garhwal-Kumaon Himalaya: A hypothetical analysis. *Int J Env Sci* 5:697
- Das Y (2015b) Some aspects of thunderstorm over India during pre-monsoon season: a preliminary report. *J Geosci Geomat* 3:68–78
- Das S, Ashrit R, Moncrieff MW (2006) Simulation of a Himalayan cloudburst event. *J Earth Syst Sci* 115:299–313
- De US, Dube RK, Rao GP (2005) Extreme weather events over India in the last 100 years. *J Ind Geophys Union* 9:173–187
- Deo AA, Ganer DW (2014) Tropical cyclone activity over the Indian Ocean in the warmer climate. In: Mohanty UC et al (eds) Monitoring and prediction of tropical cyclones in the indian ocean and climate change, pp 72–80. [https://doi.org/10.1007/978-94-007-7720-0\\_7](https://doi.org/10.1007/978-94-007-7720-0_7)
- Deshpande NR, Kothawale DR, Kumar V, Kulkarni JR (2018) Statistical characteristics of cloud burst and mini-cloud burst events during monsoon season in India. *Int J Climatol* 38:4172–4188
- Dimri AP et al (2017) Cloudbursts in Indian Himalayas: a review. *Earth-sci rev* 168:1–23
- Doswell CA (2001) Severe convective storms—an overview. Severe convective storms. American Meteorological Society, Boston, pp 1–26

- Dvorak VF (1984) Tropical cyclone intensity analysis using satellite data. NOAA technical report NESDIS 11:1–47
- Elsner JB, Kocher B (2000) Global tropical cyclone activity: a link to the North Atlantic Oscillation. *Geophys Res Lett* 27:129–132
- Elsner JB, Kossin JP, Jagger TH (2008) The increasing intensity of the strongest tropical cyclones. *Nature* 455:92–95. <https://doi.org/10.1038/nature07234>
- Emanuel K (2005) Increasing destructiveness of tropical cyclones over the past 30 years. *Nature* 436:686
- Evan AT, Kossin JP, Ramanathan V (2011) Arabian Sea tropical cyclones intensified by emissions of black carbon and other aerosols. *Nature* 479:94
- Evan AT, Kossin JP, Chung C, Ramanathan V (2012) Intensified Arabian Sea tropical storms. *Nature* 2012:E2–E3
- Ghosh A, Lohar D, Das J (2008) Initiation of Nor'wester in relation to mid-upper and low-level water vapor patterns on METEOSAT-5 images. *Atmos Res* 87:116–135
- Girishkumar MS, Ravichandran M (2012) The influences of ENSO on tropical cyclone activity in the Bay of Bengal during October–December. *J Geophys Res* 117:C02033. <https://doi.org/10.1029/2011jc007417>
- Girishkumar MS, Prakash VT, Ravichandran M (2015) Influence of Pacific Decadal oscillation on the relationship between ENSO and tropical cyclone activity in the Bay of Bengal during October–December. *Clim Dyn* 44:3469–3479
- Goswami BN et al (2006) Increasing trend of extreme rain events over India in a warming environment. *Science* 314:1442–1445
- Gray WM (1968) Global view of the origin of tropical disturbances and storms. *Mon Wea Rev* 96:669–700
- Guhathakurta P, Sreejith OP, Menon PA (2011) Impact of climate change on extreme rainfall events and flood risk in India. *J Earth Syst Sci* 120:359–373
- Gupta S, Jain I, Johari P, Lal M (2018) Impact of climate change on tropical cyclones frequency and intensity on Indian Coasts. In: Rao PJ et al (eds) *Proceedings of international conference on remote sensing for disaster management*. Springer Series in Geomechanics and Geoengineering. [https://doi.org/10.1007/978-3-319-77276-9\\_32](https://doi.org/10.1007/978-3-319-77276-9_32)
- Haggag M, Yamashita T, Kim KO, Lee HS (2010) Simulation of the North Indian ocean tropical cyclones using the regional environment simulator: application to cyclone Nargis in 2008. In: Charabi Y (eds) *Indian Ocean tropical cyclones and climate change*, pp 73–82. Springer, Dordrecht
- Houze RA, Rasmussen KL, Medina S, Brodzik SR, Romatschke U (2011) Anomalous atmospheric events leading to the summer 2010 floods in Pakistan. *Bull Am Meteorol Soc* 92:291–298
- Hoyos CD, Agudelo PA, Webster PJ, Curry JA (2006) De-convolution of the factors contributing to the increase in global hurricane intensity. *Science* 312:94–97
- Hunt KM, Turner AG, Inness PM, Parker DE, Levine DERC (2016) On the structure and dynamics of Indian monsoon depressions. *Mon Wea Rev* 144:3391–3416
- India Meteorological Department (IMD) (2003) *Cyclone Manual*. IMD, New Delhi
- IPCC (2007) *Climate change 2007: Synthesis report*. Contribution of Working Groups I, II and III to the Fourth Assessment Report of the Intergovernmental Panel on Climate Change. Geneva, Switzerland, 72 pp
- IPCC (2014) *Climate change 2014: synthesis report*. Contribution of Working Groups I, II and III to the Fifth Assessment Report of the Intergovernmental Panel on Climate Change. Geneva, Switzerland, 151 pp
- Kandalgaonkar SS, Tinmaker MIR, Nath A, Kulkarni MK, Trim-bake HK (2005) Study of thunderstorm and rainfall activity over the Indian region. *Atmosfera* 18:91–101
- Kikuchi K, Wang B (2010) Formation of tropical cyclones in the northern Indian Ocean associated with two types of tropical intra-seasonal oscillation modes. *J Meteorol Soc Jpn* 88:475–496. <https://doi.org/10.2151/jmsj.2010-313.p-0>
- Klotzbach PJ, Landsea CW (2015) Extremely intense hurricanes: revisiting Webster et al. (2005) after 10 years. *J Clim* 28:7621–7629
- Knutson TR et al (2010a) Tropical cyclones and climate change. *Nat Geosci* 3:157–163. <https://doi.org/10.1038/ngeo779>
- Knutson TR (2010b) Tropical cyclones and climate change: an Indian Ocean perspective. In: Charabi Y (ed) *Indian Ocean tropical cyclones and climate change*, pp 47–49. [https://doi.org/10.1007/978-90-481-3109-9\\_7](https://doi.org/10.1007/978-90-481-3109-9_7)
- Knutson TR et al (2014) Recent research at GFDL on surface temperature trends and simulations of tropical cyclone activity in the Indian Ocean region. In: Mohanty UC et al (eds), *Monitoring and prediction of tropical cyclones in the Indian Ocean and climate change*, pp 50–55
- Knutson TR et al (2015) Global projections of intense tropical cyclone activity for the late twenty-first century from dynamical downscaling of CMIP5/RCP4. 5 scenarios. *J Clim* 28:7203–7224
- Knutson T et al (2019a) Tropical cyclones and climate change assessment: part I. Detection and attribution. *Bull Am Meteorol Soc*. <https://doi.org/10.1175/bams-d-18-0189.1>
- Knutson T et al (2019b) Tropical cyclones and climate change assessment: Part II. Projected response to anthropogenic warming. *Bull Am Meteorol Soc*. <https://doi.org/10.1175/bams-d-18-0194.1>
- Knutson TK, Tuleya RE (2004) Impact of CO<sub>2</sub>-induced warming on simulated hurricane intensity and precipitation: sensitivity to the choice of climate model and convective parameterization. *J Clim* 17:3477–3495
- Knutson TR, Tuleya RE, Kurihara Y (1998) Simulated increase of hurricane intensities in a CO<sub>2</sub>-warmed climate. *Science* 279:1018–1020
- Knutson TR, Tuleya RE, Shen W, Ginis I (2001) Impact of CO<sub>2</sub>-induced warming on hurricane intensities as simulated in a hurricane model with ocean coupling. *J Climate* 14:2458–2468
- Knutson TR, Delworth T, Dixon K, Held I, Lu J, Ramaswamy V, Schwarzkopf M, Stenchikov G, Stouffer R (2006) Assessment of twentieth-century regional surface temperature trends using the GFDL CM2 coupled models. *J Clim* 19:1624–1651
- Kossin JP (2018) A global slowdown of tropical-cyclone translation speed. *Nature* 558:104–107
- Krishnan R et al (2016) Deciphering the desiccation trend of the South Asian monsoon hydroclimate in a warming world. *Clim Dyn* 47:1007–1027
- Krishnan R et al (2019) Unraveling climate change in the Hindu Kush Himalaya: rapid warming in the mountains and increasing extremes. In: Wester P et al (eds) *The Hindu Kush Himalaya assessment—mountains, climate change, sustainability and people*, pp 57–98
- Kulkarni JR et al (2015) Unprecedented hailstorms over north peninsular India during February–March 2014. *J Geophys Res* 120:2899–2912
- Kulkarni MK, Tinmaker MIR, Manohar GK (2009) Characteristics of thunderstorm activity over India. *Int J Meteorol* 34(344): 341
- Kumar SVJ, Ashtikar SS, Mohapatra M (2017) Life period of cyclonic disturbances over the NIO during recent years. In: Mohapatra M et al (eds) *Tropical cyclone activity over the North Indian Ocean*. Springer, Berlin 390 pp
- Litta AJ et al (2012) Simulation of tornado over Orissa (India) on March 31, 2009, using WRF–NMM model. *Nat Hazards* 61:1219–1242
- Lotus S (2015) Heavy rainfall over Jammu & Kashmir during 3–6 September, 2014 leading to flooding condition. *Monsoon 2014: a report (ESSO/IMD/ SYNOPTIC MET/01(2015)/17)*. India Meteorological Department, National Climate Center, Pune, India



- Mandal GS, Krishna P (2009) Global warming, climate change and cyclone related destructive winds—discussion of results from some selected studies with emphasis on the north Indian Ocean. *Glob Environ Res* 13:141–150
- Manohar GK, Kesarkar AP (2005) Climatology of thunderstorm activity over the Indian region: III. Latitudinal and seasonal variation. *Mausam* 56:581–592
- Manohar GK, Kandalgaonkar SS, Tinmaker MIR (1999) Thunderstorm activity over India and the Indian southwest monsoon. *J Geophys Res* 104:4169–4188
- McDonald RE et al (2005) Tropical storms: representation and diagnosis in climate models and the impacts of climate change. *Clim Dyn* 25:19–36
- Middleton NJ (1986) A geography of dust storms in South-west Asia. *J Climatol* 6:183–196
- Mishra A (2014) Temperature rise and trend of cyclones over the eastern coast of India. *J Earth Sci Clim Change* 5–9. <https://doi.org/10.4172/2157-7617.1000227>
- Mishra V, Shah HL (2018) Hydroclimatological perspective of the Kerala flood of 2018. *J Geol Soc India* 92:645–650
- Mohanty UC, Pattanayak S, Osuri KK (2010) Changes in frequency and intensity of tropical cyclones over Indian seas in a warming environment. *Disaster Dev* 4:53–77
- Mohanty UC, Osuri KK, Pattanayak S, Sinha P (2012) An observational perspective on tropical cyclone activity over Indian seas in a warming environment. *Nat Hazards* 63:1319–1335
- Mohapatra M, Bandyopadhyay BK, Tyagi A (2012) Best track parameters of tropical cyclones over the North Indian Ocean: a review. *Nat Hazards* 63:1285–1317
- Mohapatra M, Bandyopadhyay BK, Tyagi A (2014) Construction and quality of best tracks parameters for study of climate change impact on tropical cyclones over the north Indian ocean during satellite era. Monitoring and prediction of tropical cyclones in the Indian ocean and climate change. Springer, Dordrecht, pp 3–17
- Mohapatra M, Bandyopadhyay BK, Rathore LS (eds) (2017) Tropical cyclone activity over the North Indian Ocean. Springer, Berlin, 390 pp. <https://doi.org/10.1007/978-3-319-40576-6>
- Mooley DA (1980) Severe cyclonic storms in the Bay of Bengal 1877–1977. *Mon Wea Rev* 108:1647–1655
- Mooley DA, Mohile CM (1984) Cyclonic storms of the Arabian Sea, 1877–1980. *Mausam* 35:127–134
- Mukherjee S, Aadhar S, Stone D, Mishra DV (2018) Increase in extreme precipitation events under anthropogenic warming in India. *Weather Clim Extremes* 20:45–53
- Mukhopadhyay P, Singh HAK, Singh SS (2005) Two severe nor'westers in April 2003 over Kolkata, India, using Doppler radar observations and satellite imagery. *Weather* 60:343–353
- Murakami H et al (2012b) Future changes in tropical cyclone activity projected by the new high-resolution MRI-AGCM. *J Clim* 25:3237–3260
- Murakami H, Mizuta R, Shindo E (2012) Future changes in tropical cyclone activity projected by multi-physics and multi-SST ensemble experiments using the 60-km-mesh MRI-AGCM. *Clim Dyn* 39:2569–2584. <https://doi.org/10.1007/s00382-011-1223-x>
- Murakami H, Sugi M, Kitoh A (2013) Future changes in tropical cyclone activity in the North Indian Ocean projected by high-resolution MRI-AGCMs. *Clim Dyn* 40:1949–1968
- Murakami H, Sugi M, Kitoh A (2014) Future changes in tropical cyclone activity in the North Indian Ocean projected by the new high-resolution MRI-AGCM. In: Mohanty UC et al (eds) Monitoring and prediction of tropical cyclones in the Indian Ocean and climate change, pp 63–71. [https://doi.org/10.1007/978-94-007-7720-0\\_6](https://doi.org/10.1007/978-94-007-7720-0_6)
- Murakami H, Vecchi GA, Underwood S (2017) Increasing frequency of extremely severe cyclonic storms over the Arabian Sea. *Nat Clim Change* 7:885–889
- Murugavel P, Pawar SD, Gopalakrishnan V (2014) Climatology of lightning over Indian region and its relationship with convective available potential energy. *Int J Climatol* 34:3179–3187
- Niyas NT, Srivastava AK, Hatwar HR (2009) Variability and trend in the cyclonic storms over north Indian Ocean. National Climate Centre, Office of the Additional Director General of Meteorology (Research), India Meteorological Department
- Oouchi K et al (2006) Tropical cyclone climatology in a global-warming climate as simulated in a 20 km-mesh global atmospheric model: frequency and wind intensity analyses. *J Meteorol Soc Jpn* 84:259–276
- Orlanski I (1975) A rational subdivision of scales for atmospheric processes. *Bull Am Meteorol Soc* 56:527–530
- Pandey SK, Vinoy V, Landu K, Babu KSS (2017) Declining pre-monsoon dust loading over South Asia: signature of a changing regional climate. *Sci Rep* 7(1). <https://doi.org/10.1038/s41598-017-16338-w>
- Pattanaik DR (2005) Variability of oceanic and atmospheric conditions during active and inactive periods of storms over the Indian region. *Int J Climatol* 25:1523–1530
- Pielke RA et al (2005) Hurricanes and global warming. *Bull Am Meteorol Soc* 86:1571–1575
- Pradhan D, De UK, Singh UV (2012) Development of nowcasting technique and evaluation of convective indices for thunderstorm prediction in Gangetic West Bengal (India) using Doppler Weather Radar and upper air data. *Mausam* 63:299–318
- Prajeesh AG, Ashok K, Rao DVB (2013) Falling monsoon depression frequency: a Gray-Sikka conditions perspective. *Nat Scientific Rep*. <https://doi.org/10.1038/srep02989>
- Priya P, Krishnan R, Mujumdar M, Houze RA (2017) Changing monsoon and midlatitude circulation interactions over the Western Himalayas and possible links to occurrences of extreme precipitation. *Clim Dyn* 49:2351–2364
- Raghavan S, Rajesh S (2003) Trends in tropical cyclone impact—a study in Andhra Pradesh, India. *Bull Am Meteorol Soc* 84:635–644. <https://doi.org/10.1175/BAMS-84-5-635>
- Raghavendra VK (1973) A statistical analysis of the number of tropical storms and depressions in the Bay of Bengal during 1890–1969. *Ind J Meteorol Geophys* 24:125–130
- Raipal DK, Deka SN (1980) ANDHI, the convective dust storm of northwest India. *Mausam* 31:31–442
- Rajeevan M, Srinivasan J, Niranjan Kumar K, Gnanaseelan C, Ali MM (2013) On the epochal variation of intensity of tropical cyclones in the Arabian Sea. *Atmos Sci Lett* 14:249–255
- Ramesh Kumar MR, Sankar S (2010) Impact of global warming on cyclonic storms over north Indian Ocean. *Indian J Mar Sci* 39:516–520
- Ramsay H (2017) The global climatology of tropical cyclones. Oxford research encyclopedia of natural hazard science, Oxford University Press, 34 pp
- Ranalkar MR et al (2016) Incessant rainfall event of June 2013 in Uttarakhand, India: observational perspectives. In: High-impact weather events over the SAARC Region. Springer, Cham, pp 303–312
- Rao DVB, Srinivas D, Satyanarayana GC (2019) Trends in the genesis and landfall locations of tropical cyclones over the Bay of Bengal in the current global warming era. *J Earth Syst Sci* 128. <https://doi.org/10.1007/s12040-019-1227-1>
- Rasmussen KL, Houze RA (2012) A flash-flooding storm at the steep edge of high terrain: disaster in the Himalayas. *Bull Amer Meteorol Soc* 93:1713–1724

- Romatschke U, Houze RA (2011) Characteristics of precipitating convective systems in the South Asian monsoon. *J Hydrometeorol* 12:3–26
- Saha U, Maitra A, Midya SK, Das GK (2014) Association of thunderstorm frequency with rainfall occurrences over an Indian urban metropolis. *Atmos Res* 138:240–252
- Sahoo BP, Bhaskaran K (2016) Assessment on historical cyclone tracks in the Bay of Bengal, east coast of India. *Int J Climatol* 36:95–109
- Sebastian M, Behera MR (2015) Impact of SST on tropical cyclones in North Indian Ocean. *Procedia Eng* 116:1072–1077
- Sikka DR (2006) Major advances in understanding and prediction of tropical cyclones over the north Indian Ocean: a perspective. *Mausam* 57:165–196
- Singh OP (2007) Long-term trends in the frequency of severe cyclones of Bay of Bengal: observations and simulations. *Mausam* 58:59–66
- Singh O, Bhardwaj P (2019) Spatial and temporal variations in the frequency of thunderstorm days over India. *Weather* 74:138–144
- Singh OP, Khan TMA (1999) Changes in the frequencies of cyclonic storms and depressions over the Bay of Bengal and the Arabian Sea. SAARC Meteorological Research Centre Report 2, 121 pp
- Singh OP, Rout RK (1999) Frequency of cyclonic disturbances over the North Indian Ocean during ENSO years. In: *Meteorology beyond 2000: Proceedings of TROPMET-99, Chennai, India*, pp 297–301
- Singh OP, Khan TA, Rahman MS (2000) Changes in the frequency of tropical cyclones over the North Indian Ocean. *Meteorol Atmos Phys* 75:11–20
- Singh OP, Khan TMA, Rahman S (2001) Has the frequency of intense tropical cyclones increased in the north Indian Ocean? *Curr Sci* 80:575–580
- Singh C, Mohapatra M, Bandyopadhyay BK, Tyagi A (2011) Thunderstorm climatology over northeast and adjoining east India. *Mausam* 62:163–170
- Singh K, Panda J, Osuri KK, Vissa NK (2016) Progress in tropical cyclone predictability and present status in the North Indian Ocean region. In: Lupo A (ed) *in recent developments in tropical cyclone dynamics, prediction, and detection*, pp 193–215. <https://doi.org/10.5772/64333>
- Singh D, Ghosh S, Roxy MK, McDermid S (2019) Indian summer monsoon: extreme events, historical changes, and role of anthropogenic forcings. *Wiley Interdiscip Rev Clim Change* 10(2):e571
- Sugi M, Noda A, Sato N (2002) Influence of the global warming on tropical cyclone climatology: an experiment with the JMA global model. *J Meteorol Soc Jpn* 80:249–272
- Sugi M, Murakami H, Yoshimura J (2009) A reduction in global tropical cyclone frequency due to global warming. *Sola* 5:164–167
- Sugi M, Murakami H, Yoshimura J (2014) Mechanism of the Indian Ocean tropical cyclone frequency changes due to global warming. In: Mohanty UC et al (eds) *Monitoring and prediction of tropical cyclones in the Indian Ocean and climate change*, pp 40–49. [https://doi.org/10.1007/978-94-007-7720-0\\_4](https://doi.org/10.1007/978-94-007-7720-0_4)
- Sumesh KGMR, Kumar MR (2013) Tropical cyclones over north Indian Ocean during El-nino modoki years. *Nat Hazards* 68:1057–1074
- Thayyen RJ, Dimri AP, Kumar P, Agnihotri G (2013) Study of cloudburst and flash floods around Leh, India, during August 4–6, 2010. *Nat Hazards* 65:2175–2204
- Tsuboi A, Takemi T (2014) The interannual relationship between MJO activity and tropical cyclone genesis in the Indian Ocean. *Geosci Lett* 1:9. <https://doi.org/10.1186/2196-4092-1-9>
- Tyagi A (2007) Thunderstorm climatology over Indian region. *Mausam* 58:189–212
- Tyagi A, Bandyopadhyay BK, Mohapatra M (2010) Monitoring and prediction of cyclonic disturbances over North Indian ocean by regional specialised meteorological centre, New Delhi (India): problems and prospective. *Indian Ocean tropical cyclones and climate change*. Springer, Dordrecht, pp 93–103
- Tyagi A, Sikka DR, Goyal S, Bhowmick M (2012) A satellite based study of pre-monsoon thunderstorms (Nor'westers) over eastern India and their organization into mesoscale convective complexes. *Mausam* 63:29–54
- Velden C et al (2006) The Dvorak tropical cyclone intensity estimation technique: a satellite-based method that has endured for over 30 years. *Bull Am Meteorol Soc* 87:1195–1210
- Vellore RK et al (2014) On the anomalous precipitation enhancement over the Himalayan foothills during monsoon breaks. *Clim Dyn* 43:2009–2031
- Vellore RK et al (2016) Monsoon-extratropical circulation interactions in Himalayan extreme rainfall. *Clim Dyn* 46:3517–3546
- Vellore RK et al (2019) Sub-synoptic variability in the Himalayan extreme precipitation event during June 2013. *Met Atmos Phys* <https://doi.org/10.1007/s00703-019-00713-5>
- Vidale PL, Roberts M, Hodges K, Strachan J, Demory ME, Slingo J (2010) Tropical cyclones in a hierarchy of climate models of increasing resolution. In: Charabi Y (ed) *Indian Ocean tropical cyclones and climate change*. Springer, Berlin, pp 9–14
- Vishnu S, Sanjay J, Krishnan R (2019) Assessment of climatological TC activity over the North Indian Ocean in the CORDEX-South Asia regional climate models. *Clim Dyn*. <https://doi.org/10.1007/s00382-019-04852-8>
- Walsh KJ et al (2016) Tropical cyclones and climate change. *Wiley Interdiscip Rev Clim Change* 7(1):65–89
- Wang B, Xu S, Wu L (2012) Intensified Arabian Sea tropical storms. *Nature* 489:E1–E2. <https://doi.org/10.1038/nature11470>
- Webster PJ, Holland GJ, Curry JA, Chang HR (2005) Changes in tropical cyclone number, duration, and intensity in a warming environment. *Science* 309:1844–1846
- Xie S-P, Deser C, Vecchi GA, Ma J, Teng H, Wittenberg AT (2010) Global warming pattern formation: sea surface temperature and rainfall. *J Clim* 23:966–986
- Yoshimura J, Masato S, Noda A (2006) Influence of greenhouse warming on tropical cyclone frequency. *J Meteorol Soc Jpn* 84:405–428
- Yu J, Wang Y (2009) Response of tropical cyclone potential intensity over the north Indian Ocean to global warming. *Geophys Res Lett* 36. <https://doi.org/10.1029/2008gl036742>
- Zhao M, Held IM (2012) TC-permitting GCM simulations of hurricane frequency response to sea surface temperature anomalies projected for the late twenty-first century. *J Clim* 25:2995–3009
- Zhao M, Held IM, Lin S-J, Vecchi GA (2009) Simulations of global hurricane climatology, interannual variability, and response to global warming using a 50 km resolution GCM. *J Clim* 22:6653–6678

**Open Access** This chapter is licensed under the terms of the Creative Commons Attribution 4.0 International License (<http://creativecommons.org/licenses/by/4.0/>), which permits use, sharing, adaptation, distribution and reproduction in any medium or format, as long as you give appropriate credit to the original author(s) and the source, provide a link to the Creative Commons license and indicate if changes were made.

The images or other third party material in this chapter are included in the chapter's Creative Commons license, unless indicated otherwise in a credit line to the material. If material is not included in the chapter's Creative Commons license and your intended use is not permitted by statutory regulation or exceeds the permitted use, you will need to obtain permission directly from the copyright holder.

